

Aspects of Strangeness –1 Meson-Baryon Scattering

José A. Oller¹, Joaquim Prades² and Michela Verbeni¹

¹ Departamento de Física, Universidad de Murcia, E-30071 Murcia, Spain

² CAFPE and Departamento de Física Teórica y del Cosmos, Universidad de Granada, Campus de Fuente Nueva, E-18002 Granada, Spain

Received: date / Revised version: date

Abstract. We consider meson-baryon interactions in S-wave with strangeness -1 . This is a sector populated by plenty of resonances interacting in several two-body coupled channels. We consider a large set of experimental data, where the recent experiments are remarkably accurate. This requires a sound theoretical description to account for all the data and we employ Unitary Chiral Perturbation Theory up to and including $\mathcal{O}(p^2)$. The spectroscopy of our solutions is studied within this approach, discussing the rise of the two $\Lambda(1405)$ resonances and of the $\Lambda(1670)$, $\Lambda(1800)$, $\Sigma(1480)$, $\Sigma(1620)$ and $\Sigma(1750)$. We finally argue about our preferred fit.

PACS. 13.75.Jz Kaon-baryon interactions – 12.39.Fe Chiral Lagrangians – 11.80.-m Relativistic scattering theory – 11.80.Gw Multichannel scattering

1 Introduction

The study of strangeness -1 meson-baryon dynamics comprising the $\bar{K}N$ plus coupled channels, has been renewed both from theoretical and experimental sides. Experimentally, we have new exciting data like the increasing improvement in precision of the measurement of the α line of kaonic hydrogen accomplished recently by DEAR [1], and its foreseen better determination, with an expected error of a few eV, by the DEAR/SIDDHARTA Collaboration [2]. This has established a challenge to theory in order to match such precision. In this respect, ref.[3] provides an improvement over the traditional Deser formula for relating scattering at threshold with the spectroscopy of hadronic atoms [4]. In addition, one needs a good scattering amplitude to be implemented in this equation. The study of strangeness -1 meson-baryon scattering has a long history [5, 6, 7, 8, 9, 10, 11, 12] within K-matrix models, dispersion relations, meson-exchange models, quark models, cloudy bag-models or large N_c QCD, just to quote a few. However, in more recent years it has received a lot of attention from the application of SU(3) baryon Chiral Perturbation Theory (CHPT) to this sector together with a unitarization procedure, see e.g., [13, 14, 15, 16, 17, 18, 19, 20, 21, 22]. Recently, ref.[3] pointed out the possible inconsistency of the DEAR measurement on kaonic hydrogen and K^-p scattering, since the unitarized CHPT results, able to reproduce the scattering data, were not in agreement with DEAR. Later on, ref.[20] insisted on this fact based on its own fits, although they only included partially the $\mathcal{O}(p^2)$ CHPT amplitudes [21]. However, the

situation changed with ref.[22], as it was shown that one can obtain fits in Unitary CHPT (UCHPT), including full $\mathcal{O}(p^2)$ CHPT amplitudes, which are compatible both with DEAR and with K^-p scattering data. In addition, ref.[23] extended the work of ref.[22] by including additional experimental data, recently measured with remarkable precision by the Crystal Ball Collaboration, for the reactions $K^-p \rightarrow \eta\Lambda$ [24] and $\pi^0\pi^0\Sigma^0$ [25]. The importance of including the latter data in any analysis of K^-p interactions has been singled out in ref.[26]. We will report here about the series of works [22, 21, 23] on meson-baryon CHPT. Recently, we also presented the first full and minimal SU(3) CHPT meson-baryon Lagrangians to $\mathcal{O}(p^3)$ in ref.[27].

The study of K^-p plus coupled channel interactions offers, from the theoretical point of view, a very challenging test ground for chiral effective field theories of QCD since one has there plenty of experimental data, Goldstone bosons dynamics and large and explicit SU(3) breaking. In addition, this sector shows a very rich spectroscopy with many I=0, 1 S-wave resonances that will be the object of our study as well. Apart from that, these interactions are interrelated with many other interesting areas, e.g., possible kaon condensation in neutron-proton stars, large yields of K^- in heavy ions collisions, kaonic atoms or non-zero strangeness content of the proton.

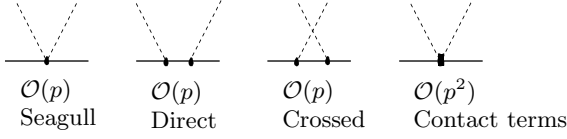


Fig. 1. Diagrams for the calculation of the baryon CHPT scattering amplitudes up to and including $\mathcal{O}(p^2)$. The first three diagrams are of $\mathcal{O}(p)$ while the last one is of $\mathcal{O}(p^2)$.

2 Formalism and Results

A general meson-baryon partial wave in coupled channels can be written in matrix notation as [17],

$$T = [1 + \mathcal{K}g]^{-1} \mathcal{K} , \quad (1)$$

where g is a diagonal matrix that comprises the unitarity bubble for every channel and \mathcal{K} is the interaction kernel that is determined from meson-baryon CHPT. This is accomplished by performing a power expansion of T calculated from CHPT and then matched, order by order, with the chiral expansion of eq.(1),

$$T_1 + T_2 + T_3 + \mathcal{O}(p^4) = \mathcal{K}_1 + \mathcal{K}_2 + \mathcal{K}_3 - \mathcal{K}_1 \cdot g \cdot \mathcal{K}_1 + \mathcal{O}(p^4) , \quad (2)$$

taking into account that g is of chiral order one. We calculate \mathcal{K} up to $\mathcal{O}(p^2)$, $\mathcal{K}_1 = T_1$ and $\mathcal{K}_2 = T_2$. The lowest order result, T_1 , contains the seagull, direct and crossed exchange diagrams, while the next-to-leading order amplitudes, T_2 , come from pure contact interactions. This is shown diagrammatically in fig.1. Once the kernel $\mathcal{K} = T_1 + T_2$ has been calculated, we insert it in eq.(1) and evaluate the S-wave amplitudes.

In ref.[22] a large set of meson-baryon scattering data was fitted which was enlarged in ref.[23] including new precise ones from the Crystal Ball Collaboration. Namely, ref.[22] took into account the $\sigma(K^-p \rightarrow K^-p)$ elastic cross section [29,30,31,32], the $\sigma(K^-p \rightarrow \bar{K}^0 n)$ charge exchange one [29,30,32,33,34], and several hyperon production reactions, $\sigma(K^-p \rightarrow \pi^+ \Sigma^-)$ [29,30,31], $\sigma(K^-p \rightarrow \pi^- \Sigma^+)$ [30,31,32], $\sigma(K^-p \rightarrow \pi^0 \Sigma^0)$ [30] and $\sigma(K^-p \rightarrow \pi^0 \Lambda)$ [30]. In our normalization the corresponding cross section, keeping only the S-wave, is given by

$$\sigma(K^-p \rightarrow MB) = \frac{1}{16\pi s} \frac{p'}{p} |T_{K^-p \rightarrow MB}|^2 , \quad (3)$$

where MB denotes the final meson-baryon system, p' the final CM three-momentum and p the initial one.

Table 1. A-type fits that agree with the DEAR data, eq.(5). The $\sigma_{\pi N}$ value enforced in the fits is given in the first row. For precise definitions of the parameters f , b_0 , b_D , b_F , b_i and a_i see ref.[23]. Three among the parameters b_0 , b_D , b_F and b_i are fixed.

Units	$\sigma_{\pi N}$ MeV	20*	30*	40*
MeV	f	75.2	71.8	67.8
GeV ⁻¹	b_0	-0.615	-0.750	-0.884
GeV ⁻¹	b_D	+0.818	+0.848	+0.873
GeV ⁻¹	b_F	-0.114	-0.130	-0.138
GeV ⁻¹	b_1	+0.660	+0.670	+0.676
GeV ⁻¹	b_2	+1.144	+1.169	+1.189
GeV ⁻¹	b_3	-0.297	-0.316	-0.315
GeV ⁻¹	b_4	-1.048	-1.181	-1.307
	a_1	-1.786	-1.591	-1.413
	a_2	-0.519	-0.454	-0.386
	a_5	-1.185	-1.170	-1.156
	a_7	-5.251	-5.209	-5.123
	a_8	-1.316	-1.310	-1.308
	a_9	-1.186	-1.132	-1.050

In addition, we also fit the precisely measured ratios at the K^-p threshold [35,36]:

$$\gamma = \frac{\sigma(K^-p \rightarrow \pi^+ \Sigma^-)}{\sigma(K^-p \rightarrow \pi^- \Sigma^+)} = 2.36 \pm 0.04 , \quad (4)$$

$$R_c = \frac{\sigma(K^-p \rightarrow \text{charged particles})}{\sigma(K^-p \rightarrow \text{all})} = 0.664 \pm 0.011 ,$$

$$R_n = \frac{\sigma(K^-p \rightarrow \pi^0 \Lambda)}{\sigma(K^-p \rightarrow \text{all neutral states})} = 0.189 \pm 0.015.$$

The first two ratios, which are Coulomb corrected, are measured with 1.7% precision, which is of the same order as the expected isospin violations. Indeed, all the other observables we fit have uncertainties larger than 5%.

Since we are just considering the S-wave amplitudes, we only include in the fits those data points for the several K^-p cross sections with laboratory frame K^- three-momentum $p_K \leq 0.2$ GeV. This also enhances the sensitivity to the lowest energy region in which we are particularly interested. We also include in the fits the $\pi^\pm \Sigma^\mp$ event distributions from the chain of reactions $K^-p \rightarrow \Sigma^+(1660)\pi^-$, $\Sigma^+(1660) \rightarrow \pi^+ \Sigma\pi$ [37].

The number of data points included in each fit, without the data for the energy shift and width of kaonic hydrogen, is 97. Unless the opposite is stated, we also include in the fits the DEAR measurement of the shift and width of the 1s kaonic hydrogen energy level [1],

$$\begin{aligned} \Delta E &= 193 \pm 37(stat) \pm 6(syst.) \text{ eV}, \\ \Gamma &= 249 \pm 111(stat.) \pm 39(syst.) \text{ eV}, \end{aligned} \quad (5)$$

which is around a factor of two more precise than the KEK previous measurement [28], $\Delta E = 323 \pm 63 \pm 11$ eV and $\Gamma = 407 \pm 208 \pm 100$ eV. To calculate the shift and width of the 1s kaonic hydrogen state we use the results of [3] incorporating isospin breaking corrections up

Table 2. Table of results of the A-type fits, given in table 1. The $\sigma_{\pi N}$ value enforced in the fits is given in the first row.

$\sigma_{\pi N}$	20*	30*	40*
γ	2.36	2.36	2.37
R_c	0.629	0.628	0.628
R_n	0.168	0.171	0.173
ΔE (eV)	194	192	192
Γ (eV)	324	302	270
ΔE_D (eV)	204	204	207
Γ_D (eV)	361	338	305
a_{K^-p} (fm)	$-0.49 + i 0.44$	$-0.49 + i 0.41$	$-0.50 + i 0.37$
a_0 (fm)	$-1.07 + i 0.53$	$-1.04 + i 0.50$	$-1.02 + i 0.45$
a_1 (fm)	$0.44 + i 0.15$	$0.40 + i 0.15$	$0.33 + i 0.14$
$\delta_{\pi\Lambda}(\Xi)$ ($^\circ$)	3.4	4.5	5.7
m_0 (GeV)	1.2	1.1	1.0
a_{0+}^+ ($10^{-2} \cdot M_\pi^{-1}$)	-2.0	-2.2	-2.2

to and including $\mathcal{O}(\alpha^4, (m_d - m_u)\alpha^3)$. We further constrain our fits by computing at $\mathcal{O}(p^2)$ in baryon SU(3) CHPT several πN observables with the values of the low energy constants involved in the fit. Unitarity corrections in the πN sector are not as large as in the $S = -1$ sector, e.g., there isn't anything like a $\Lambda(1405)$ resonance close to threshold, and hence a calculation within pure SU(3) baryon CHPT is more reliable here. Thus, we calculate at $\mathcal{O}(p^2)$, a_{0+}^+ , the isospin-even pion-nucleon S-wave scattering length, $\sigma_{\pi N}$, the pion-nucleon σ term, and m_0 from the value of the proton mass m_p . In this way we fix three of our free parameters.

Table 3. B-type fits that do not agree with the DEAR data, eq.(5). The enforced $\sigma_{\pi N}$ value in the fit is shown in the first line. For precise definitions of the parameters f , b_0 , b_D , b_F , b_i and a_i see ref.[23]. Three among the parameters b_0 , b_D , b_F and b_i are fixed.

Units	$\sigma_{\pi N}$ MeV	20*	30*	40*	$\mathcal{O}(p)$
MeV	f	95.8	113.2	100.0	93.9
GeV $^{-1}$	b_0	-0.201	-0.159	-0.487	0*
GeV $^{-1}$	b_D	-0.005	-0.297	0.127	0*
GeV $^{-1}$	b_F	-0.133	-0.157	-0.188	0*
GeV $^{-1}$	b_1	+0.122	+0.016	+0.135	0*
GeV $^{-1}$	b_2	-0.080	-0.151	-0.037	0*
GeV $^{-1}$	b_3	-0.533	-0.281	-0.494	0*
GeV $^{-1}$	b_4	+0.028	-0.291	-0.173	0*
	a_1	+4.037	+4.188	+2.930	-2.958
	a_2	-2.063	-3.129	-2.400	-1.479
	a_5	-1.131	-1.214	-1.225	-1.330
	a_7	-3.488	-3.000	-2.795	-1.805
	a_8	-0.347	+0.642	+2.906	-0.655
	a_9	-1.767	-2.109	-1.913	-1.918

In addition ref.[23] included further data from recent experiments of the Crystal Ball Collaboration [24,25]. These data comprises the $K^-p \rightarrow \eta\Lambda$ cross section and $\Sigma\pi$ event distributions from the reaction $K^-p \rightarrow \pi^0\pi^0\Sigma^0$. As noted in ref.[23] these data cannot be reproduced from the fits

given in ref.[22] and then new fits were considered in the former reference that from the beginning included the data from [24,25]. As in ref.[22] two type of fits were found. The so called A-type fits, table 1, that together with scattering data also reproduce the DEAR measurement on kaonic hydrogen, and the B-type fits, table 3, that reproduce the former but not the latter. In fig.2 and table 2 we show the reproduction of the data by the A-type fits and in fig.3 and table 4 the same is done for the B-type fits. In the last column of table 3 we include the lowest order fit, only with \mathcal{K}_1 , also shown in fig.3.

It is worth stressing the good reproduction of the data accomplished by the A-type fits, including the most recent measurement of the kaon hydrogen lowest energy level and width. One also observes a factor of 2 of difference between the K^-p scattering lengths of the A- and B-type fits. So, if finally the DEAR measurement [1] is confirmed by the results of the DEAR/SIDDHARTA Collaboration [2], it would give rise to an important step forward in the knowledge of kaon-nucleon interactions. This difference in the scattering lengths makes also that only the A-type fits have a pattern of isospin violation in the calculations of the shift and width of kaonic hydrogen of expected size [3]. For the B-type fits the isospin violations turn out to be rather large, 30%, while for the A-type only 14%. In addition, we also observe from tables 2 and 4 that the values of the scattering lengths are rather independent of the values given to the sigma terms.

3 Spectroscopy

We show in tables 5 and 6 the I=0 and 1 poles, respectively, corresponding to the so-called fit I of ref.[23], given in the fifth column of table 1.

By passing continuously from one Riemann sheet to the other some of the poles in the tables with the same isospin are connected and represent the same resonance. One observes poles corresponding to the $\Lambda(1405)$, $\Lambda(1670)$ and $\Lambda(1800)$ in good agreement with the mass and width given to those resonances in the PDG [38]. In addition, there is a lighter resonance around 1310 MeV, not quoted

Table 4. Table of results for the B-type fits, given in table 3.

$\sigma_{\pi N}$	20*	30*	40*	$\mathcal{O}(p)$
γ	2.34	2.35	2.34	2.32
R_c	0.643	0.643	0.644	0.637
R_n	0.160	0.163	0.176	0.193
ΔE (eV)	436	409	450	348
Γ (eV)	614	681	591	611
ΔE_D (eV)	418	385	436	325
Γ_D (eV)	848	880	844	775
a_{K-p} (fm)	$-1.01 + i 1.03$	$-0.93 + i 1.07$	$-1.06 + i 1.02$	$-0.79 + i 0.94$
a_0 (fm)	$-1.75 + i 1.15$	$-1.65 + i 1.30$	$-1.79 + i 1.10$	$-1.50 + i 1.00$
a_1 (fm)	$-0.13 + i 0.39$	$-0.14 + i 0.36$	$-0.12 + i 0.46$	$0.32 + i 0.46$
$\delta_{\pi\Lambda}(\Xi)$ ($^\circ$)	-1.4	1.7	-1.2	-1.4
m_0 (GeV)	0.8	0.6	0.7	-
a_{0+}^+ ($10^{-2} \cdot M_\pi^{-1}$)	-0.5	-1.4	+0.3	-

Table 5. Fit I, I=0 Poles. The pole positions are given in MeV and the couplings in GeV. The symbol $|\gamma_i|_I$ means the coupling of the corresponding pole to the state with definite isospin I made up by the charged states of the i_{th} channel. The couplings to the I=1, 2 channels are always close to zero.

Re(Pole)	-Im(Pole)	Sheet	$ \gamma_{\pi\Lambda} $	$ \gamma_{\pi\Sigma} _0$	$ \gamma_{\pi\Sigma} _1$	$ \gamma_{\pi\Sigma} _2$	$ \gamma_{\bar{K}N} _0$	$ \gamma_{\bar{K}N} _1$	$ \gamma_{\eta\Lambda} $	$ \gamma_{\eta\Sigma} $	$ \gamma_{K\Xi} _0$	$ \gamma_{K\Xi} _1$
1301	13	1RS	0.03	1.12	0.02	0.01	5.83	0.05	0.41	0.04	2.11	0.03
1309	13	2RS	0.02	3.66	0.02	0.02	4.46	0.04	0.21	0.04	3.05	0.03
1414	23	2RS	0.14	4.24	0.13	0.01	4.87	0.39	0.85	0.20	9.35	0.11
1388	17	3RS	0.02	3.81	0.02	0.02	1.33	0.04	0.42	0.04	9.55	0.04
1676	10	3RS	0.01	1.28	0.03	0.00	1.67	0.01	2.19	0.07	5.29	0.07
1673	18	4RS	0.01	1.26	0.02	0.00	1.82	0.01	2.13	0.06	5.32	0.06
1825	49	5RS	0.02	2.29	0.02	0.00	2.10	0.02	0.89	0.03	7.43	0.09

Table 6. Fit I, I=1 Poles. The pole positions are given in MeV and the couplings in GeV. The couplings to the I=0, 2 channels are always close to zero. The notation is like in table 5.

Re(Pole)	-Im(Pole)	Sheet	$ \gamma_{\pi\Lambda} $	$ \gamma_{\pi\Sigma} _0$	$ \gamma_{\pi\Sigma} _1$	$ \gamma_{\pi\Sigma} _2$	$ \gamma_{\bar{K}N} _0$	$ \gamma_{\bar{K}N} _1$	$ \gamma_{\eta\Lambda} $	$ \gamma_{\eta\Sigma} $	$ \gamma_{K\Xi} _0$	$ \gamma_{K\Xi} _1$
1425	6.5	2RS	1.35	0.24	1.66	0.01	0.35	3.92	0.05	4.23	0.49	2.98
1468	13	2RS	2.80	0.16	5.96	0.02	0.23	8.74	0.04	10.66	0.19	2.48
1433	3.7	3RS	0.65	0.08	0.80	0.00	0.12	1.58	0.02	5.82	0.20	2.14
1720	18	4RS	1.82	0.02	1.21	0.00	0.02	0.95	0.02	6.78	0.05	5.31
1769	96	6RS	2.65	0.00	0.61	0.00	0.00	2.48	0.00	3.32	0.01	4.22
1340	143	3-4RS	1.33	0.14	5.50	0.02	0.02	1.58	0.00	3.28	0.03	1.20
1395	311	3-4RS	2.08	0.01	1.49	0.01	0.00	1.24	0.00	7.63	0.01	3.97

Fig. 2. The solid lines correspond to the $\sigma = 40^*$ MeV fit, the dashed lines to the 30^* MeV fit, and the dash-dotted curves to the 20^* MeV one of table 1. The different lines can be barely distinguished. For experimental references see ref.[23].

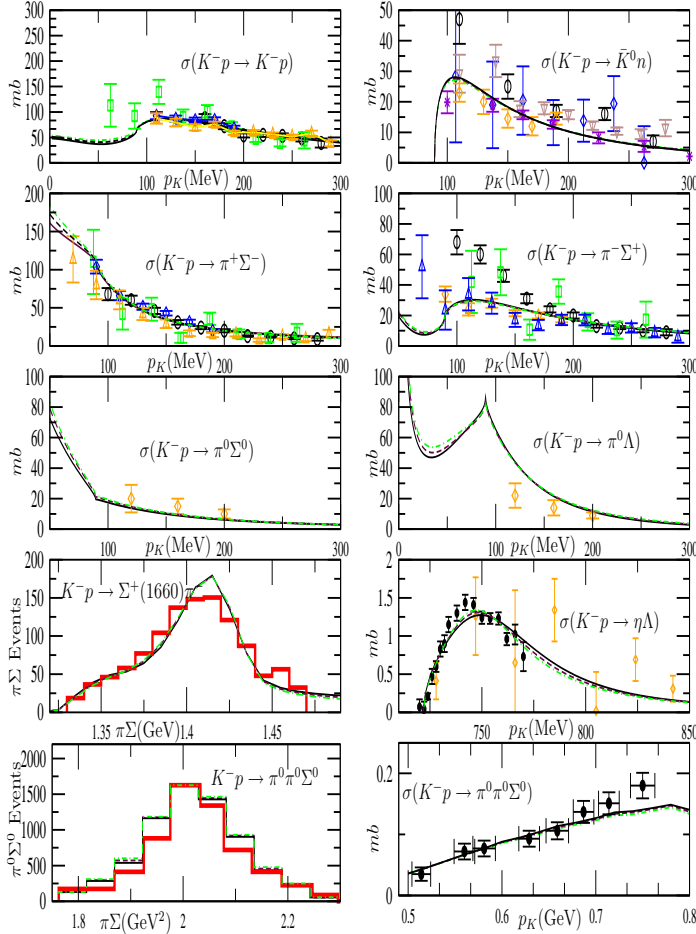
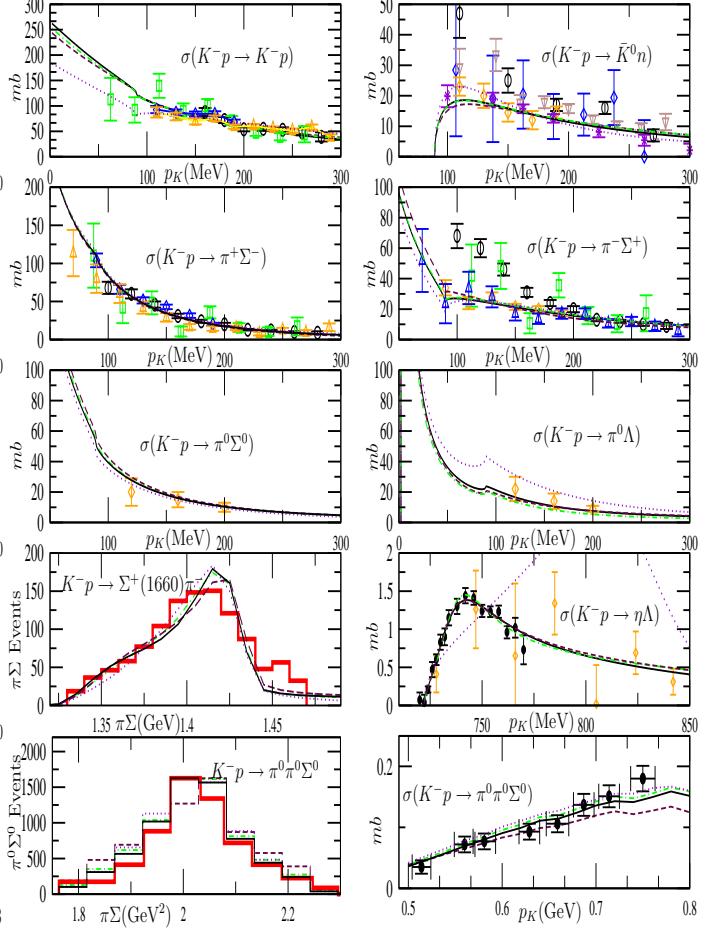


Fig. 3. The solid lines correspond to the $\sigma_{\pi N} = 40^*$ MeV fit, the dashes lines to the 30^* MeV fit, the dash-dotted curves to the 20^* MeV one and the dotted lines to the $\mathcal{O}(p)$ fit of table 3.



in the PDG, and this has to do with the so called two $\Lambda(1405)$ resonances, although for fit I it appears much lighter than in ref.[18]. For $I=1$ one has the $\Sigma(1750)$ resonance. Fit I amplitudes also show in $I=1$ a broad bump at around 1.6 GeV corresponding to the $\Sigma(1620)$. There are also other poles around the $\bar{K}N$ threshold which mix up giving rise to a clear bump structure from 1.4 to 1.45 GeV. These poles could be related to the $\Sigma(1480)$ [39]. Finally, we also observe an $I=2$ pole for fit I at $1722 - i 181$ MeV.

In tables 7 and 8 the $I=0, 1$ poles positions for the fit II of ref.[23], given in the fifth column of table 4, are shown. There are also poles corresponding to the $\Lambda(1405)$, $\Lambda(1670)$ but not for the $\Lambda(1800)$. There is no $\Sigma(1750)$ resonance either and the bumps for the $\Sigma(1620)$ have disappeared in several amplitudes.

In summary we have reviewed the works of refs.[22, 21, 23]. We have shown two types of fits that agree with scat-

tering experimental data but only one type agrees with the DEAR measurement of kaonic hydrogen [1]. These latter fits are also those that offer a remarkable agreement with spectroscopic information [38]. Hence, taken into consideration the present experimental information, the so called fits A, table 1, are preferred over the fits B, table 3.

This work has been supported in part by the MEC (Spain) and FEDER (EC) Grants Nos. FPA2003-09298-C02-01 (J.P.), FPA2004-03470 (J.A.O. and M.V.), the Fundación Séneca grant Ref. 02975/PI/05 (J.A.O. and M.V.), the European Commission (EC) RTN Network EURIDICE under Contract No. HPRN-CT2002-00311 and the Hadron-Physics I3 Project (EC) Contract No RII3-CT-2004-506078 (J.A.O.) and by Junta de Andalucía Grants Nos. FQM-101 (J.P. and M.V.) and FQM-347 (J.P.).

Table 7. Fit II, I=0 Poles. The pole positions are given in MeV and the couplings in GeV. The notation is like in table 5.

Re(Pole)	-Im(Pole)	Sheet	$ \gamma_{\pi\Lambda} $	$ \gamma_{\pi\Sigma} _0$	$ \gamma_{\pi\Sigma} _1$	$ \gamma_{\pi\Sigma} _2$	$ \gamma_{\bar{K}N} _0$	$ \gamma_{\bar{K}N} _1$	$ \gamma_{\eta\Lambda} $	$ \gamma_{\eta\Sigma} $	$ \gamma_{K\Xi} _0$	$ \gamma_{K\Xi} _1$
1347	36	2RS	0.02	6.48	0.12	0.02	2.60	0.10	1.42	0.01	0.32	0.07
1427	18	2RS	0.12	3.87	0.23	0.01	6.99	0.23	3.49	0.05	1.64	0.32
1340	41	3RS	0.07	5.92	0.08	0.01	0.62	0.08	2.33	0.01	0.75	0.04
1667	8	4RS	0.03	0.77	0.05	0.00	0.59	0.01	3.32	0.02	12.17	0.08
1667	8	5RS	0.03	0.77	0.05	0.00	0.59	0.01	3.32	0.03	12.17	0.06

Table 8. Fit II, I=1 Poles. The pole positions are given in MeV and the couplings in GeV. The notation is like in table 5.

Re(Pole)	-Im(Pole)	Sheet	$ \gamma_{\pi\Lambda} $	$ \gamma_{\pi\Sigma} _0$	$ \gamma_{\pi\Sigma} _1$	$ \gamma_{\pi\Sigma} _2$	$ \gamma_{\bar{K}N} _0$	$ \gamma_{\bar{K}N} _1$	$ \gamma_{\eta\Lambda} $	$ \gamma_{\eta\Sigma} $	$ \gamma_{K\Xi} _0$	$ \gamma_{K\Xi} _1$
1399	41	2RS	1.49	0.09	5.58	0.01	0.13	4.92	0.08	0.73	0.03	4.99
1424	3.6	2RS	0.54	0.14	1.58	0.00	0.20	1.17	0.10	0.61	0.04	3.76
1311	122	3-4RS	2.63	0.05	4.61	0.01	0.02	3.44	0.02	0.60	0.03	3.60
1426	3	3RS	0.56	0.04	1.18	0.00	0.07	0.77	0.04	0.61	0.02	3.74

References

- G. Beer *et al.* [DEAR Collaboration], Phys. Rev. Lett. **94**, (2005) 212302.
- D. L. Sirghi and F. Sirghi, (DEAR/SIDDHARTA Collaboration), The physics of kaonic atoms at DAFNE, http://www.lnf.infn.it/esperimenti/dear/DEAR_RPR.pdf.
- U.-G. Meißner, U. Raha and A. Rusetsky, Eur. Phys. J. **C35**, (2004) 349.
- S. Deser *et al.*, Phys. Rev. **96**, (1954) 774; T. L. Trueman, Nucl. Phys. **26**, (1961) 57.
- R. H. Dalitz and S. F. Tuan, Phys. Rev. Lett. **2**, (1959) 425; Ann. Phys. **8**, (1959) 100.
- A. D. Martin, N. M. Queen and G. Violini, Nucl. Phys. **B10**, (1969) 481; P. M. Gensini, R. Hurtado and G. Violini, PiN Newslett. **13**, (1997) 291; B. Di Claudio, A. M. Rodriguez-Vargas and G. Violini, Z. Phys. **C3**, (1979) 75.
- A. D. Martin, Nucl. Phys. **B179**, (1979) 33.
- R. Buttgen, K. Holinde and J. Speth, Phys. Lett. **B163**, (1985) 305; R. Buettgen, K. Holinde, A. Mueller-Groeling, J. Speth and P. Wyborny, Nucl. Phys. **A506**, (1990) 586; A. Mueller-Groeling, K. Holinde and J. Speth, Nucl. Phys. **A513**, (1990) 557.
- T. Hamaie, M. Arima and K. Masutani, Nucl. Phys. **A591**, (1995) 675
- P. J. Fink, G. He, R. H. Landau and J. W. Schnick, Phys. Rev. **C41**, (1990) 2720.
- E. A. Veit, B. K. Jennings, R. C. Barrett and A. W. Thomas, Phys. Lett. **B 137**, (1984) 415.
- J. L. Goity, C. L. Schat and N. N. Scoccola, Phys. Rev. **D66**, (2002) 114014; Phys. Rev. Lett. **88**, (2002) 102002.
- N. Kaiser, P. B. Siegel and W. Weise, Nucl. Phys. **A594**, (1995) 325.
- J. A. Oller and E. Oset, Nucl. Phys. **A620**, (1997) 438; (*E*)-*ibid.* **A652**, (1999) 407.
- E. Oset and A. Ramos, Nucl. Phys. **A635**, (1998) 99.
- J. A. Oller, E. Oset and A. Ramos, Prog. Part. Nucl. Phys. **45**, (2000) 157.
- J. A. Oller and U.-G. Meißner, Phys. Lett. **B500**, (2000) 263.
- D. Jido, J. A. Oller, E. Oset, A. Ramos and U.-G. Meißner, Nucl. Phys. **A725**, (2003) 181.
- C. Garcia-Recio, M. F. M. Lutz and J. Nieves, Phys. Lett. **B582**, (2004) 49.
- B. Borasoy, R. Nissler and W. Weise, Phys. Rev. Lett. **94**, (2005) 213401; *Ibid.* **96**, (2006) 199201; Eur. Phys. J. **A25**, (2005) 79; Phys. Rev. **C74**, (2006) 055201. arXiv:hep-ph/0606108.
- J. A. Oller, J. Prades and M. Verbeni, Phys. Rev. Lett. **96** (2006) 199202.
- J. A. Oller, J. Prades and M. Verbeni, Phys. Rev. Lett. **95**, (2005) 172502.
- J. A. Oller, Eur. Phys. J. **A28**, (2006) 63.
- A. Starostin *et al.* [Crystal Ball Collaboration], Phys. Rev. **C64**, (2001) 055205.
- S. Prakhov *et al.* [Crystal Ball Collaboration], Phys. Rev. **C70**, (2004) 034605.
- V. K. Magas, E. Oset and A. Ramos, Phys. Rev. Lett. **95**, (2005) 052301.
- J. A. Oller, M. Verbeni and J. Prades, J. High Energy Phys **09**, (2006) 079; (E)-hep-ph/0701096; M. Frink, U.-G. Meißner, Eur. Phys. J. **A29**, (2006) 255.
- M. Iwasaki *et al.*, Phys. Rev. Lett. **78**, (1997) 3067; Phys. Rev. **C58**, (1998) 2366.
- W. E. Humphrey and R. R. Ross, Phys. Rev. **127**, (1962) 1305.

30. J.K. Kim, Phys. Rev. Lett. **14**, (1965) 29.
31. M. Sakitt *et al.*, Phys. Rev. **139**, (1965) B719.
32. J. Ciborowski *et al.*, J. Phys. **G8**, (1982) 13.
33. W. Kittel, G. Otter and I. Wacek, Phys. Lett. **21**, (1966) 349.
34. D. Evans *et al.*, J. Phys. **G9**, (1983) 885.
35. R.J. Nowak *et al.*, Nucl. Phys. **B139**, (1978) 61.
36. D. Tovee *et al.*, Nucl. Phys. **B33**, (1971) 493.
37. R.J. Hemmingway, Nucl. Phys. **B253**, (1985) 742.
38. W. M. Yao *et al.* [Particle Data Group], J. Phys. **G33** (2006) 1.
39. I. Zychor *et al.*, Phys. Rev. Lett. **96**, (2006) 012002.